

The bony labyrinth in the Aroeira 3 Middle Pleistocene cranium

Mercedes Conde-Valverde ^{a,*}, Rolf Quam ^{a,b,c,d}, Ignacio Martínez ^{a,c},
Juan-Luis Arsuaga ^{a,c,e}, Joan Daura ^f, Montserrat Sanz ^{c,e}, João Zilhão ^{g,h,i}



^a Grupo de Investigación en Bioacústica Evolutiva y Paleoantropología, Área de Antropología Física, Departamento de Ciencias de la Vida, Universidad de Alcalá, 28871 Alcalá de Henares, Madrid, Spain

^b Department of Anthropology, Binghamton University (SUNY), Binghamton, NY 13902-6000, USA

^c Centro Mixto (UCM-ISCIH) de Evolución y Comportamiento Humanos, Av. Monforte de Lemos 5, 28029 Madrid, Spain

^d Division of Anthropology, American Museum of Natural History, Central Park West-79th St., New York, NY 10024, USA

^e Departamento de Geodinámica, Estratigrafía y Paleontología, Facultad de Ciencias Geológicas, Universidad Complutense de Madrid, 28040 Madrid, Spain

^f Grup de Recerca del Quaternari (GRQ)-SERP, Departament d'Història i Arqueologia, C/ Montalegre 6-8, 08007 Barcelona, Spain

^g UNIAHQ-Centro de Arqueologia da Universidade de Lisboa, Faculdade de Letras, Universidade de Lisboa, Alameda da Universidades, 1600-214 Lisbon, Portugal

^h Departament d'Història i Arqueologia, Universitat de Barcelona, 08007 Barcelona, Spain

ⁱ Institució Catalana de Recerca i Estudis Avançats (ICREA), Passeig Lluís Companys 23, 08010 Barcelona, Spain

ARTICLE INFO

Article history:

Received 25 April 2018

Accepted 13 August 2018

Keywords:

Evolution
Inner ear
Temporal bone
Neandertal
Atapuerca
Iberian Peninsula

ABSTRACT

The discovery of a partial cranium at the site of Aroeira (Portugal) dating to 389–436 ka augments the current sample of Middle Pleistocene European crania and makes this specimen penecontemporaneous with the fossils from the geographically close Atapuerca Sima de los Huesos (SH) and Arago sites. A recent study of the cranium documented a unique combination of primitive and derived features. The Aroeira 3 cranium preserves the right temporal bone, including the petrosal portion. Virtual reconstruction of the bony labyrinth from μ CT scans provides an opportunity to examine its morphology. A series of standard linear and angular measures of the semicircular canals and cochlea in Aroeira 3 were compared with other fossil hominins and recent humans. Our analysis has revealed the absence of derived Neandertal features in Aroeira 3. In particular, the specimen lacks both the derived canal proportions and the low position of the posterior canal, two of the most diagnostic features of the Neandertal bony labyrinth, and Aroeira 3 is more primitive in these features than the Atapuerca (SH) sample. One potentially derived feature (low shape index of the cochlear basal turn) is shared between Aroeira 3 and the Atapuerca (SH) hominins, but is absent in Neandertals. The results of our study provide new insights into Middle Pleistocene population dynamics close to the origin of the Neandertal clade. In particular, the contrasting inner ear morphology between Aroeira 3 and the Atapuerca (SH) hominins suggests a degree of demographic isolation, despite the close geographic proximity and similar age of these two sites.

1. Introduction

The European Middle Pleistocene is one of the most contentious periods in paleoanthropology, especially in terms of the evolutionary relationships between the fossils found in Africa and Europe. This situation is partly due to the fact that the Middle Pleistocene hominin record has long suffered from poor chronological control for key specimens, and the contrasting morphologies

observed in these fossils have clouded our understanding of the evolutionary process during this period.

Some authors prefer to group some European Middle Pleistocene fossils (e.g., Petralona, Mauer, Arago) with those from Africa (e.g., Kabwe, Bodo) into a single widespread, variable species, most often referred to as *Homo heidelbergensis* (Rightmire, 2008; Tattersall, 2011; Stringer, 2012). Focusing on the European fossil record, the recent analysis of the large sample of fossils from the Atapuerca (SH) site has revealed the presence of two main groups of fossils in the European Middle Pleistocene (Arsuaga et al., 2014).

On the one hand, there is a series of fossils, including Mauer, Arago, Ceprano and Mala Balanica, that lack clear Neandertal

* Corresponding author.

E-mail address: mercedes.conde@edu.uah.es (M. Conde-Valverde).

derived traits (Roksandic et al., 2011; de Lumley, 2015; Manzi, 2016), and which could reasonably be included in *H. heidelbergensis*. On the other hand, there is a series of fossils such as those from the sites of Atapuerca (SH), Swanscombe, Steinheim and Reilingen that show some clearly derived Neandertal features in their anatomy (Dean et al., 1998; Stringer and Hublin, 1999; Arsuaga et al., 2014) and, in the case of the Atapuerca (SH) hominins, in their nuclear DNA (Meyer et al., 2016). This anatomical and genetic evidence indicates that this latter group belongs to the same clade as the Neandertals of the Late Pleistocene.

Nevertheless, the full suite of Neandertal features only emerges towards the end of the Middle Pleistocene, perhaps around 200 ka (Hublin, 2009). The Atapuerca (SH) hypodigm, and by extension these other European Middle Pleistocene specimens, is sufficiently different from the Late Pleistocene Neandertals to be separated at least as different paleodemes (Martínez and Arsuaga, 1997; Tattersall, 2011; Arsuaga et al., 2014). Whether this difference is on the specific or subspecific level is currently an open question (Arsuaga et al., 2014). Regardless of the precise taxonomic allocation of these fossils, the existence of these two morphological groupings in the European Middle Pleistocene, one with a more primitive morphology and one with more clear affinities with the Neandertals, is recognized by many researchers (Tattersall, 2011; Stringer, 2012; Arsuaga et al., 2014; Manzi, 2016).

In this context, the recent discovery of a partial cranium from the Middle Pleistocene site of the Gruta da Aroeira (Portugal) is particularly relevant since it augments the still small non-SH European Middle Pleistocene sample (Daura et al., 2017). The Gruta da Aroeira is one of a series of Pleistocene archaeological and paleontological sites located in the Almonda karst system (Torres Novas). The Aroeira site was previously excavated between 1997 and 2002 and was designated as “Galerias Pesadas” (Marks et al., 2002a,b), while the more recent phase of fieldwork was resumed in 2013. The Aroeira site has yielded abundant archaeological materials, including Acheulean handaxes and three human fossils (Aroeira 1–3). Aroeira 1 and 2 are represented by isolated teeth (Trinkaus et al., 2003), while Aroeira 3 is a partial cranium (Daura et al., 2017). Three stratigraphic units have been identified at the Aroeira site, and the cranium was found in Unit 2 encased in very hard breccia. In addition, several hundred stone tools were recovered from this same unit (Daura et al., 2018), along with fragmentary and some burnt faunal remains. The age of the cranium was estimated relying on several radiometric dating techniques and likely falls between 389 and 436 ka, making Aroeira 3 one of the best dated crania from the European Middle Pleistocene and approximately contemporaneous with the Atapuerca (SH) sample (Daura et al., 2017).

In a recent study of the Aroeira 3 cranium, Daura et al. (2017) showed that it presents a unique combination of primitive and derived features among European Middle Pleistocene fossils. Based on the morphology of the glabellar and mastoid regions, as well as the presence of a well-developed postglenoid process, these authors concluded that Aroeira 3 was similar to the fossils from the Atapuerca (SH) site, Bilzingsleben and Steinheim. On the other hand, Daura et al. (2017) also indicated that the current evidence from the European Middle Pleistocene fossil hominin record is difficult to reconcile with a linear evolutionary model, and they suggested the existence of complex population dynamics, including population replacement, isolation and hybridization.

Although the Aroeira 3 cranium is incomplete, the right temporal bone, including the petrosal portion, is intact, providing the opportunity to examine its bony labyrinth morphology. Variation in bony labyrinth morphology among modern human populations has recently been shown to reflect population history below the species level (Ponce de León et al., 2018). In fossil hominins, the bony

labyrinth has been shown to contain phylogenetic information, and species-specific differences have been reported previously (Spoor, 1993; Spoor et al., 2003). In particular, Neandertals show several derived features in the bony labyrinth, including the relative canal proportions, a low position of the posterior canal, and distinct angular relationships of the lateral canal with the surrounding petrosal bone elements. While this suite of features occurs at high frequencies in Neandertals, some of the individual features can occasionally be found in other groups as well. In particular, fossils from two sites in China (Xujiayao and Xuchang) resemble Neandertals in the low position of the posterior canal and the canal proportions (Wu et al., 2014; Li et al., 2017). In the case of Xuchang, the additional presence of a suprainiac fossa in the occipital bone led Li et al. (2017) to suggest some degree of gene flow from Neandertal populations.

A recent study of the bony labyrinth in the Atapuerca (SH) hominins has provided insights into the emergence of these derived features during the course of evolution of the Neandertal clade (Quam et al., 2016). The Atapuerca (SH) hominins already show the derived canal proportions of Neandertals (Quam et al., 2016). While a few individuals do show a low placement of the posterior canal, most of the sample does not, differing from Neandertals in this regard. In addition, the Atapuerca (SH) hominins show a low shape index of the cochlear basal turn, due to a shortened cochlear height, and this may represent a derived feature in this sample. Limited data for other non-SH European Middle Pleistocene specimens suggest that these individuals largely show the derived canal proportions and lack a low placed posterior canal (except for Reilingen; Spoor et al., 2003; Quam et al., 2016). Thus, changes in the canal proportions apparently preceded the appearance of the low placement of the posterior canal in Neandertal evolution. Given their close geographic proximity and similar chronology, comparison of the Aroeira 3 and Atapuerca (SH) bony labyrinth may provide insights into hominin evolution at or near the origin of the Neandertal clade.

2. Materials and methods

2.1. Comparative samples

The bony labyrinth in Aroeira 3 is compared with a large sample of Pleistocene and recent humans (Table 1). Comparison with the Atapuerca SH sample is of particular interest, given the close similarity in chronology and geographic location between the SH site and Aroeira. Several additional European Middle Pleistocene individuals, as well as a sample of Neandertals, help to elucidate the phylogenetic affinities of Aroeira 3. In addition, the limited data for Early and Middle Pleistocene individuals from Africa and Asia are also included to provide information on earlier members of the genus *Homo*. Some authors prefer to separate these African and Asian specimens into two distinct species (*Homo ergaster*, in the case of Africa, and *Homo erectus*, in the case of Asia; Wood, 1991; Tattersall, 2007), while others prefer to recognize all these fossils as representing a single geographically widespread species (*H. erectus*; Rightmire, 1990; Antón, 2003). We have grouped these fossils together into a single sample of *H. ergaster/H. erectus*, since previous studies have suggested that a broadly similar bony labyrinth morphology, interpreted as reflecting the primitive condition for the genus *Homo*, characterizes all of these fossils (Spoor et al., 2003; Gilbert et al., 2008; Quam et al., 2016). Two sites in China, Xujiayao and Xuchang, have yielded fossils whose taxonomic affinities are currently unclear, but for which data on the bony labyrinth are available (Wu et al., 2014; Li et al., 2017). Finally, samples of fossil and recent *Homo sapiens* were also included in the comparative analyses.

Table 1
Fossil and recent hominin samples used in the present study.

Sample	n	Specimen	Source
<i>H. erectus/H. ergaster</i>	7	Swartkrans (SK 847), Olduvai Gorge (OH 9), Sangiran 2, 4, Daka, ^a Lantian, Hexian	Spoor (1993), Gilbert et al. (2008), Wu et al. (2014)
Atapuerca (SH)	14	Cranium 3, 4, 5, 6, 7, 8, 9, 11, 12, 13, 14, 15, 17, AT-1907	Quam et al. (2016)
Middle Pleistocene Europe Neandertals	4	Abri Suard, Reilingen, Steinheim, Biache-Saint-Vaast 2	Spoor et al. (2003), Guipert et al. (2011)
	27	Arcy-sur-Cure, Dederiyeh, Gibraltar 1, 2, La Chapelle, La Ferrassie 1, 2,3, 8, La Quina 5, H27, Le Moustier 1, Pech de l'Azé, Petit Puymoyen 5, Spy 1, 2, Tabun 1, Obi-Rakhmat (OR-1) Krapina 38.1, 38.12, 38.13, 39.1, 39.4, 39.8, 39.13, 39.18, 39.20	Hublin et al. (1996), Spoor et al. (2003), Glantz et al. (2008), Hill et al. (2014), Gómez-Olivencia et al. (2015)
Xujiayao	1	Xujiayao 15	Wu et al. (2014)
Xuchang	2	Xuchang 1, 2	Li et al. (2017)
Fossil <i>H. sapiens</i>	11	Liujiang 1, Qafzeh 6, Skhul 5, Pester a cu Oase 2, Pester a Muierii, Nazlet Khater 2, Abri Pataud 1, Abri Pataud 3, Cro Magnon 1, Laugerie Basse 1, Lagar Velho, Cioclovina	Spoor et al. (2002, 2003), Bouchneb and Crevecoeur (2009), Ponce de Leon and Zollikofer (2010, 2013), Wu et al. (2014), Uhl et al. (2016)
Recent <i>H. sapiens</i>	26	Cementerio San José (n = 7), Sepulveda (n = 8), AMNH (n = 4), NESPOS (n = 7)	Quam et al. (2016)
Aroeira	1	Aroeira 3	Present study

Abbreviations: AMNH = American Museum of Natural History; NESPOS = Neanderthal Studies Professional Online Service.

^a Daka measurements refer to the high resolution data set in Gilbert et al. (2008).

2.2. Measurement protocol

We followed previously established protocols for the bony labyrinth measurements (Spoor, 1993; Spoor et al., 2003). A series of linear distances, angular relationships and indices (Fig. 1) were measured and calculated from a microCT scan of Aroeira 3. Measurements were taken with Mimics[®] v.17 (Materialise, Leuven,

Belgium), which allows for simultaneous 2D views of the individual CT scans in the sagittal, coronal and transverse planes, as well as the resulting 3D model. The diameters of the canals and cochlear basal turn were taken at the midpoint of the lumen and used to calculate the corresponding radii and shape indices and canal proportions. The angular measures were taken relative to the plane of the lateral canal and projected onto the sagittal plane. Finally, the sagittal

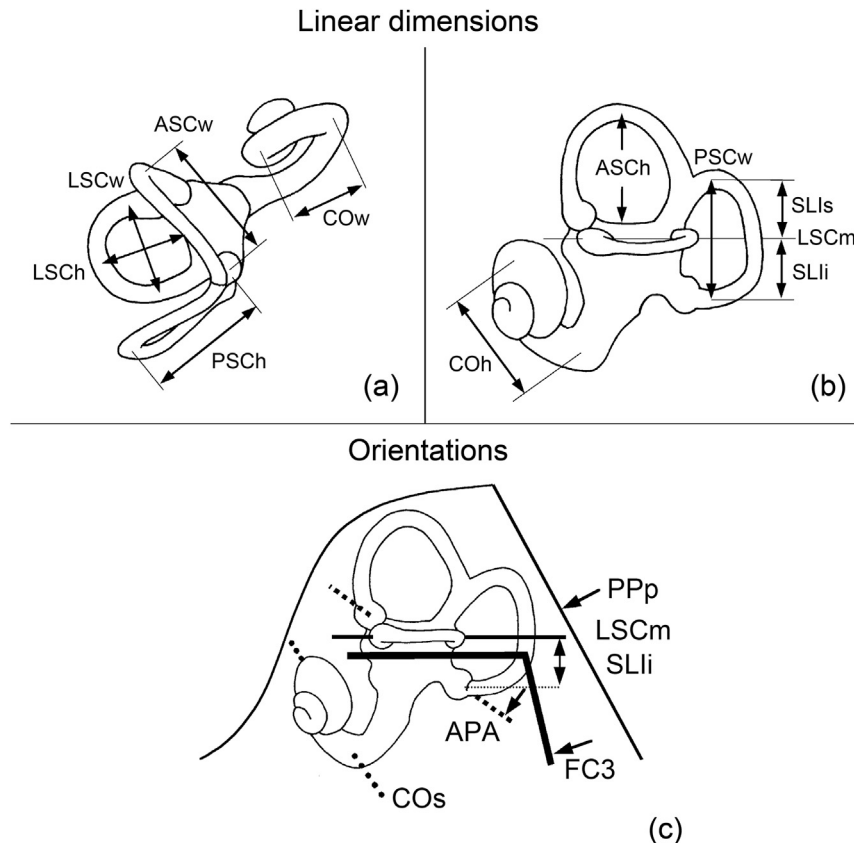


Figure 1. Superior (a) and lateral (b) aspects of a left human labyrinth, and lateral aspect (c) with the petrosal contour included showing the measurements and orientations used in the study. Abbreviations: APA = ampullar line; ASCh = height of the anterior semicircular canal; ASCw = width of the anterior semicircular canal; COh = height of the basal turn of the cochlea; COs = basal turn of the cochlea in the sagittal plane; COw = width of the basal turn of the cochlea; FC3 = third part of the facial canal in the sagittal plane; LSCch = height of the lateral semicircular canal; LSCm = arc of the lateral semicircular canal at its greatest width in the sagittal plane; LSCw = width of the lateral semicircular canal; Ppp = posterior petrosal surface in the sagittal plane at the level of the common crus; PSCh = height of the posterior semicircular canal; PSCw = width of the posterior semicircular canal; SLI = sagittal labyrinthine index, calculated from the width of the posterior canal above (SLIs) and below (SLli) the plane of the lateral canal. Definitions of the measurements and orientations are in Spoor et al. (2003). Figure modified from Spoor et al. (2003).

labyrinthine index (SLI) was calculated to quantify the position of the posterior canal relative to the plane of the lateral canal.

2.3. Statistical analysis

In addition to descriptive statistics for all of the metric variables, principal components analysis (PCA) and discriminant function analysis (DFA) were carried out using the Statistica v.10 software package (StatSoft, 2010). Since the radii of the three canals and cochlear basal turn are direct measures of size, the geometric mean of these four variables was calculated. We found no statistical correlation ($p < 0.05$) between the geometric mean and any of the remaining variables, indicating no allometric effects. Thus, the radii of the canals and cochlea were omitted from the PCA, and only those variables that reflect the shape and spatial relationships of the semicircular canals and cochlea were included: shape indices of the canals (ASC h/w, PSC h/w, LSC h/w) and cochlea (CO h/w), the sagittal labyrinthine index (SLI), the proportion of each canal (ASC%R, PSC%R, LSC%R) and the angular measures (LSCm < APA, LSCm < FC3, LSCm < Ppp, Cos < LSCm). The PCA was carried out on the correlation matrix of the included variables. The PCA was performed on a subset of the entire sample due to missing data in the literature.

The DFA was performed using cross-validation and including the same variables as the PCA (i.e., radii of the canals and cochlea were omitted) to statistically identify the most likely group membership for the Aroeira 3 specimen. DFA was carried out on the *H. ergaster/H. erectus*, Atapuerca (SH), Neandertals and recent *H. sapiens* samples. Aroeira 3, along with the non-SH European Middle Pleistocene specimens, fossil *H. sapiens* and Xujiayao 15 were not included in the calculation of the DFA. Rather, these specimens were treated as ‘unknown’ individuals, whose group membership was predicted based on the discriminant function and assuming that these unknown cases belong to one of the groups defined a priori. The DFA assumed equal prior probabilities of group membership since the differences in sample size are not reflective of an underlying difference in population size (Kachigan, 1991).

2.4. CT scanning

MicroCT scanning of the Aroeira 3 temporal bone was carried out at the Centro Nacional de Investigación sobre la Evolución Humana (CENIEH) in Burgos, Spain using a GE Phoenix v/tome/x

microCT scanner. A total of 601 slices were obtained as a 2024×2024 matrix and 8 bit gray-scale and saved in TIFF format. Scanning parameters were the following: isometric voxel size = 0.039 mm, field of view (FOV) = 78.92 mm, voltage = 130 kV, and current = 500 μ A. Virtual reconstruction of the bony labyrinth was made using the Mimics[®] software program. For those areas of the bony labyrinth that were free from matrix, we performed a semiautomatic segmentation relying on the half maximum height (HMH) thresholding protocol. The limit between bone and air was calculated as the mean of the maximum and minimum gray scale values along a profile line that crosses the bone and air boundary. Manual segmentation was necessary in those areas where the fossil was filled with sediment and semiautomatic procedures could not be applied.

3. Results

3.1. Semicircular canals

The virtual reconstruction of Aroeira 3 (Fig. 2; Supplementary Online Material (SOM) File S1) shows the size and orientations of the semicircular canals and cochlea. In both absolute (ASC-R) and relative (ASC%R) size, the anterior canal in Aroeira 3 falls within one SD of the mean in most of the comparative samples, except for the SH hominins (Table 2). While the absolute size of the anterior canal in Aroeira 3 falls towards the very upper end of the variation in the Atapuerca (SH) hominins and other European Middle Pleistocene specimens, the relative size of the canal is very similar to the means in these samples (Fig. 3). The low value for the shape index (ASC h/w) in Aroeira 3 falls within the range of variation in only the fossil *H. sapiens* and *H. ergaster/H. erectus* samples, and is mainly attributable to Aroeira 3 having a wider canal.

The absolute (PSC-R) and relative (PSC%R) sizes of the posterior canal in Aroeira 3 fall outside the range of variation in the Atapuerca (SH) hominins and other European Middle Pleistocene specimens, but are within one SD of the mean in the remaining comparative samples (Table 2; Fig. 3). The shape index (PSC h/w) is within one SD of the means in all the comparative samples but falls closest to the Atapuerca (SH) and Neandertal sample means.

The absolute size (LSC-R) of the lateral canal is within one SD of the means in all of the comparative groups, but the relative size (LSC%R) in Aroeira 3 is at the lower end of the Neandertal and Atapuerca (SH) ranges of variation and outside the values in other

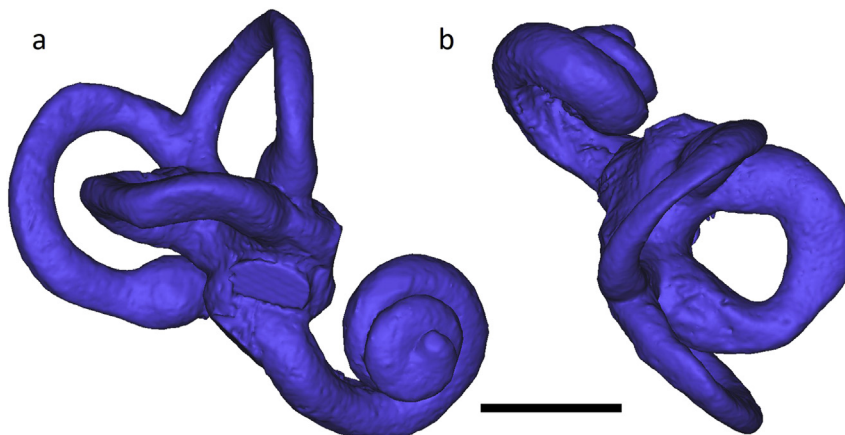


Figure 2. Lateral (a) and superior (b) views of the 3D virtual reconstruction of the Aroeira 3 bony labyrinth. The lateral view is aligned according to the plane of the lateral semicircular canal, while the superior view is aligned perpendicular to the plane of the lateral semicircular canal. Scale bar = 5 mm.

Table 2
Size and shape of the semicircular canals and sagittal labyrinthine index (SLI) in the comparative sample and Aroeira 3.

	Radii of curvature (mm)			Relative size (%)			Shape indices			SLI
	PSC-R			PSC%R			PSC h/w			
	ASC-R	PSC-R	LSC-R	ASC%R	PSC%R	LSC%R	ASC h/w	PSC h/w	LSC h/w	
Aroeira 3	3.2	3	2.5	36.5	34.6	28.9	79.7	98.2	92.7	47.0
<i>H. ergaster/H. erectus</i> mean ± SD	3.1 ± 0.2	2.9 ± 0.3	2.3 ± 0.3	37.4 ± 0.9	34.9 ± 2.1	27.8 ± 2.6	85.3 ± 11.5	104.9 ± 7.6	83.1 ± 10.6	49.2 ± 6.7
<i>H. ergaster/H. erectus</i> range (n)	2.8–3.5 (7)	2.5–3.3 (7)	2.0–2.9 (7)	36.5–39.2 (7)	32.5–38.8 (7)	23.5–30.6 (7)	69.7–104.9 (7)	95.4–114.6 (7)	62.5–92.6 (7)	41.4–61.0 (7)
Middle Pleistocene Europe mean ± SD	3.0 ± 0.1	2.7 ± 0.0	2.5 ± 0.1	36.3 ± 0.7	33.3 ± 1.0	30.4 ± 0.9	94.3 ± 3.3	110.9 ± 15.2	89.8 ± 5.7	50.3 ± 10.0
Middle Pleistocene Europe range (n)	2.8–3.1 (4)	2.7–2.7 (4)	2.3–2.6 (4)	35.4–36.9 (4)	32.1–34.2 (4)	29.1–31.0 (4)	90.0–98.0 (4)	96.0–132.0 (4)	84.0–97.1 (4)	40.0–60.0 (3)
Atapuerca (SH) mean ± SD	2.9 ± 0.2	2.6 ± 0.1	2.5 ± 0.2	36.4 ± 1.1	32.9 ± 0.8	30.7 ± 1.1	96.1 ± 5.6	100.9 ± 6.0	95.9 ± 6.3	49.2 ± 7.1
Atapuerca (SH) range (n)	2.7–3.3 (14)	2.4–2.9 (14)	2.3–2.7 (14)	34.3–38.0 (14)	31.5–34.3 (14)	28.9–32.8 (14)	87.2–107.2 (14)	88.4–111.0 (14)	85.0–105.7 (14)	36.1–60.9 (14)
Neandertals mean ± SD	3.0 ± 0.2	2.8 ± 0.2	2.6 ± 0.2	35.9 ± 1.3	33.7 ± 1.6	30.4 ± 1.3	92.7 ± 5.6	101.9 ± 7.8	92.0 ± 5.8	63.4 ± 5.7
Neandertals range (n)	2.7–3.4 (26)	2.2–3.4 (25)	2.3–2.9 (26)	33.8–39.0 (25)	28.6–35.8 (25)	28.0–32.5 (25)	84.0–103.0 (25)	87.0–115.0 (24)	83.0–105.0 (25)	53.0–76.0 (25)
Fossil <i>H. sapiens</i> mean ± SD	3.3 ± 0.2	3.0 ± 0.3	2.5 ± 0.2	37.5 ± 1.2	33.7 ± 1.7	28.9 ± 1.3	86.3 ± 8.8	103.4 ± 10.9	91.7 ± 6.1	45.7 ± 7.5
Fossil <i>H. sapiens</i> range (n)	3.0–3.6 (11)	2.5–3.3 (10)	2.2–2.8 (11)	36.0–39.5 (10)	30.6–35.9 (10)	27.2–31.8 (10)	72.0–98.4 (9)	88.0–118.0 (9)	82.0–104.3 (10)	33.0–55.1 (11)
Recent <i>H. sapiens</i> mean ± SD	3.1 ± 0.2	3.1 ± 0.3	2.3 ± 0.2	36.5 ± 1.2	36.3 ± 1.3	27.2 ± 1.6	89.2 ± 5.0	103.2 ± 5.9	93.8 ± 8.0	50.6 ± 5.4
Recent <i>H. sapiens</i> range (n)	2.5–3.6 (26)	2.4–3.6 (26)	1.9–2.7 (26)	34.2–39.0 (26)	33.5–38.6 (26)	25.0–30.5 (26)	80.3–97.3 (26)	92.4–116.3 (26)	78.1–108.0 (26)	38.9–61.1 (26)

Measurement abbreviations as in Figure 1.

European Middle Pleistocene specimens (Table 2; Fig. 3). Thus, Aroeira 3 does not show the relative enlargement of the lateral canal seen in specimens from the Neandertal clade (Spoor et al., 2003; Quam et al., 2016). The shape index of the lateral canal (LSC h/w) in Aroeira 3 is within one SD of the mean in most of the comparative samples, but falls just outside the range of variation in the *H. ergaster/H. erectus* sample. Interestingly, this is the only variable that was found to show a statistical difference between the *H. ergaster/H. erectus* sample and recent *H. sapiens* (Quam et al., 2016), and Aroeira 3 resembles recent humans in this feature.

Considering the relative proportions of all three canals (Fig. 3), all of the samples are characterized by a predominance of the anterior canal, followed by the posterior canal, with the lateral canal being the relatively smallest (Table 2). Some variability is present in individual specimens, with Xuchang 2, two Neandertals and 38.5% of the modern human sample showing a relatively larger posterior canal compared with the anterior. Neandertals are characterized by a relatively smaller posterior canal and relatively larger lateral canal when compared with *H. sapiens*, a condition also present in the Atapuerca (SH) hominins. Indeed, the relative sizes of the posterior and lateral canals in both the Atapuerca (SH) sample and Neandertals have been shown to be significantly different from *H. ergaster/H. erectus* and recent humans (Quam et al., 2016). These apparently derived canal proportions seen in Neandertals are also found in other European Middle Pleistocene fossils and the Chinese specimen Xujiayao 15. The canal proportions in Aroeira 3 are most similar to those in the *H. ergaster/H. erectus* sample as well as fossil *H. sapiens* (Fig. 3), indicating that this individual does not show the derived canal proportions seen in European specimens of the Neandertal clade.

3.2. Relative position of the posterior canal

The value for the sagittal labyrinthine index (SLI) in Aroeira 3 (47.0) falls within one SD of the mean in all of the comparative samples, except for Neandertals (Table 2). Previously, the SLI in Neandertals has been shown to differ statistically from the *H. ergaster/H. erectus*, Atapuerca (SH) and recent *H. sapiens* samples (Quam et al., 2016). The SLI in Aroeira 3 falls outside of the Neandertal range of variation (Fig. 4), indicating that the posterior canal in Aroeira 3 is not located in a low position relative to the lateral canal plane. The value in Aroeira 3 is, however, very close to that predicted (47.9) based on the size of its posterior canal (Spoor et al., 2003).

3.3. Basal turn of the cochlea

The radius of the cochlear basal turn (CO-R) in Aroeira 3 is within one SD of the mean values in all of the comparative samples (Table 3), which do not differ statistically from one another (Quam et al., 2016). In contrast, the shape index of the cochlear basal turn (CO h/w) is very low in Aroeira 3, falling outside the lower limit of the range of variation in all of the fossil comparative samples, except the Atapuerca (SH) hominins (Table 3, Fig. 4). Aroeira 3 is close to the Atapuerca (SH) mean, which has been shown to be significantly different from that of the Neandertals (Quam et al., 2016), and a low value appears to be a derived feature in the Atapuerca (SH) cochlea. Nevertheless, several fossil and recent individuals fall within the Atapuerca (SH) range of variation. Among other European Middle Pleistocene specimens, a low value is also seen in Reilingen, but among the recent *H. sapiens*, only a single individual shows a value smaller than in Aroeira 3.

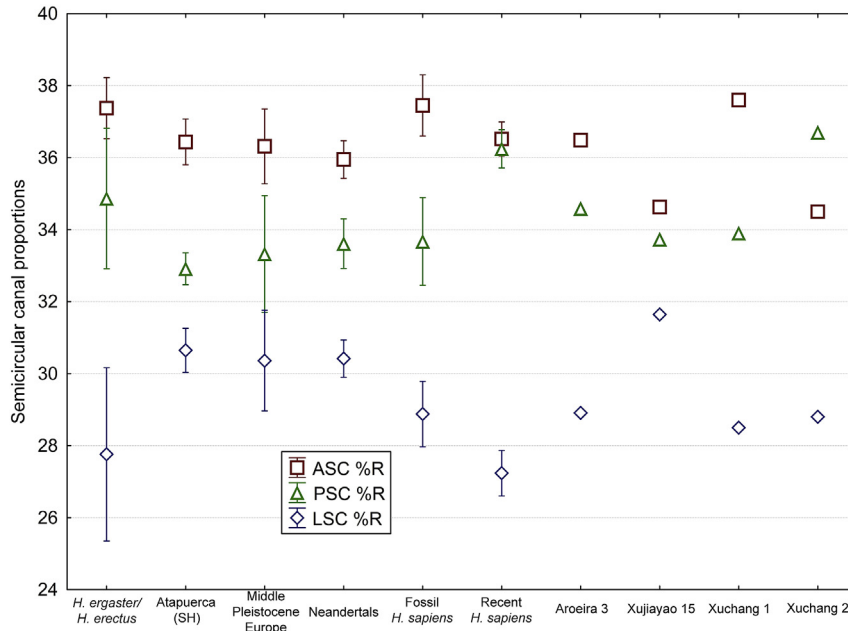


Figure 3. Box and whisker plot showing the relative proportions of the semicircular canals in Aroeira 3 compared with fossil and recent members of the genus *Homo*. Abbreviations: ASC%R = relative size of the anterior semicircular canal; LSC%R = relative size of the lateral semicircular canal; PSC%R = relative size of the posterior semicircular canal.

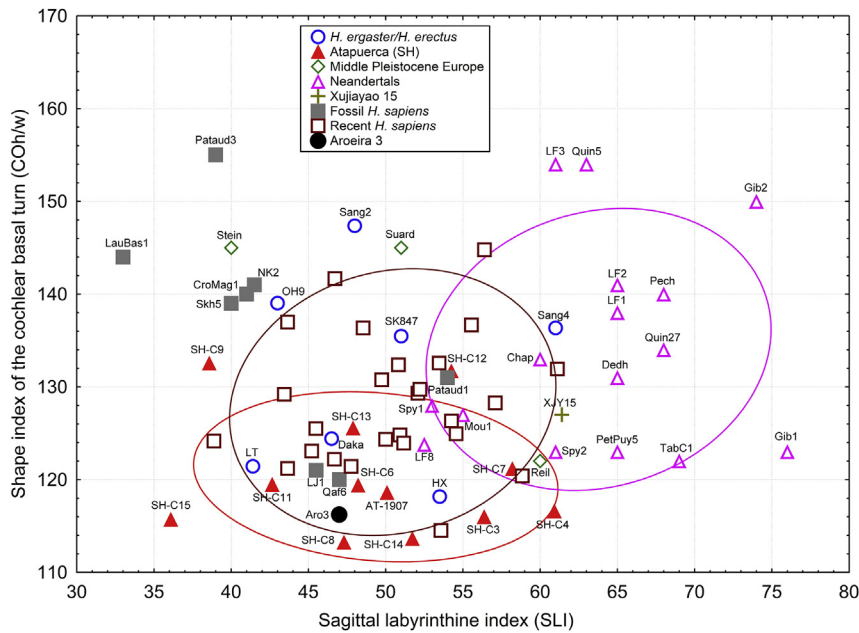


Figure 4. Scatterplot of the shape index of the cochlear basal turn (CO h/w) vs. the sagittal labyrinthine index (SLI). The 95% confidence ellipses are shown for recent *H. sapiens*, Neandertals and the Atapuerca (SH) sample and the individuals fossil specimens included in the analysis are labeled.

3.4. Angular measurements

The inclination of the ampullar line (LSCm < APA) in Aroeira 3 is within one SD of the mean in all of the comparative samples, except the Neandertals, which show considerably higher values, reflecting a more steeply inclined ampullar line (Table 4). The angle formed between the third part of the facial canal and the plane of the lateral canal (LSCm < FC3) in Aroeira 3 falls outside the lower limit of the range of variation in Neandertals and non-SH European Middle Pleistocene specimens (Table 4). While Aroeira 3 is just within the Atapuerca (SH) range of variation, it is within one SD of the fossil

and recent *H. sapiens* means. A previous study found these two angles in Neandertals to differ significantly from *H. ergaster/H. erectus*, Atapuerca (SH) and recent humans (Quam et al., 2016). The angle formed between the posterior surface of the petrous pyramid and the lateral canal (LSCm < PpP) in Aroeira falls within one SD from the means in all the comparative samples (Table 4). Higher values for these three angles are associated with a low position of the posterior canal (i.e., high SLI; Spoor et al., 2003). Finally, the angle of the cochlear basal turn (Cos < LSCm) is very high in Aroeira 3, falling within the upper limit of the range of variation in only *H. ergaster/H. erectus* and Neandertals (Table 4).

Table 3
Size and shape of the cochlear basal turn in comparative sample and Aroeira 3.

	CO-R	CO h/w
Aroeira 3	2.3	116.2
<i>H. ergaster/H. erectus</i> mean \pm SD	2.3 \pm 0.3	131.8 \pm 10.6
<i>H. ergaster/H. erectus</i> range (<i>n</i>)	1.8–2.6 (7)	118.2–147.4 (7)
Middle Pleistocene Europe mean \pm SD	2.2 \pm 0.1	137.3 \pm 13.3
Middle Pleistocene Europe range (<i>n</i>)	2.1–2.3 (3)	122.0–145.0 (3)
Atapuerca (SH) mean \pm SD	2.2 \pm 0.1	120.3 \pm 6.5
Atapuerca (SH) range (<i>n</i>)	2.1–2.5 (12)	113.3–132.6 (12)
Neandertals mean \pm SD	2.3 \pm 0.2	134.7 \pm 11.2
Neandertals range (<i>n</i>)	2.0–2.5 (15)	122.0–154.0 (15)
Fossil <i>H. sapiens</i> mean \pm SD	2.4 \pm 0.2	136.4 \pm 11.8
Fossil <i>H. sapiens</i> range (<i>n</i>)	2.2–2.7 (8)	120.0–155.0 (8)
Recent <i>H. sapiens</i> mean \pm SD	2.3 \pm 0.2	128.4 \pm 7
Recent <i>H. sapiens</i> range (<i>n</i>)	2.0–2.6 (26)	114.5–144.8 (26)

Measurement abbreviations as in Figure 1.

Table 4
Angular measures of the lateral canal in comparative sample and Aroeira 3.

	Angles (degrees)			
	LSCm < APA	LSCm < FC3	LSCm < PpP	Cos < LSCm
Aroeira 3	37.6	71.4	64.5	67.7
<i>H. ergaster/H. erectus</i> mean \pm SD	36.7 \pm 5.1	74.7 \pm 3.1	64.7 \pm 7.3	57.0 \pm 7.3
<i>H. ergaster/H. erectus</i> range (<i>n</i>)	32.1–45.0 (6)	71.0–78.0 (6)	56.0–73.0 (6)	48.9–68.0 (6)
Middle Pleistocene Europe mean \pm SD	37.1 \pm 3.9	83.7 \pm 9.1	61.7 \pm 6.8	48.2 \pm 5.6
Middle Pleistocene Europe range (<i>n</i>)	33.0–40.0 (3)	74.0–92.0 (3)	54.0–67.0 (3)	43.0–54.0 (3)
Atapuerca (SH) mean \pm SD	35.4 \pm 4.6	77.2 \pm 6.8	63.7 \pm 4.3	53.4 \pm 7.6
Atapuerca (SH) range (<i>n</i>)	28.2–42.0 (12)	68.0–90.0 (13)	59.0–71.0 (10)	36.6–61.4 (12)
Neandertals mean \pm SD	46.7 \pm 4.7	91.1 \pm 8.4	69.0 \pm 6.7	58.7 \pm 6.3
Neandertals range (<i>n</i>)	40.0–53.0 (15)	81.0–104.0 (9)	61.0–82.0 (10)	46.0–68.0 (15)
Fossil <i>H. sapiens</i> mean \pm SD	34.5 \pm 4.3	77.1 \pm 8.4	60.3 \pm 10.5	56.9 \pm 2.9
Fossil <i>H. sapiens</i> range (<i>n</i>)	29.0–42.0 (7)	63.5–86.0 (6)	51.0–80.0 (7)	52.0–60.0 (7)
Recent <i>H. sapiens</i> mean \pm SD	36.3 \pm 4.0	70.7 \pm 6.7	59.4 \pm 6.5	55.9 \pm 5.5
Recent <i>H. sapiens</i> range (<i>n</i>)	29.1–42.6 (26)	58.7–83.3 (26)	44.8–69.9 (25)	41.2–65.6 (26)

Measurement abbreviations as in Figure 1.

Table 5
Results of the principal components analysis based on the correlation matrix of bony labyrinth variables that reflect the shape and spatial relationships of the semicircular canals and cochlea.

	PC1	PC2	PC3	PC4	PC5
% total variance	28.4	16.7	12.6	10.6	9.4
Eigenvalue	3.41	2.00	1.51	1.27	1.13
ASC h/w	-0.481542	0.440856	0.572088	0.201549	0.030245
PSC h/w	-0.032134	0.027810	0.562913	-0.520423	-0.112149
LSC h/w	-0.076625	0.508065	0.664643	0.147307	-0.053889
CO h/w	0.044469	-0.233804	0.092889	-0.712067	-0.295331
SLI	-0.810384	-0.324910	0.180250	0.114298	0.009780
ASC%R	0.377727	-0.036779	0.095610	0.407157	-0.792404
PSC%R	0.432630	-0.707525	0.340929	-0.073637	0.288522
LSC%R	-0.597915	0.633553	-0.351332	-0.177782	0.220108
LSCm < PpP	-0.635520	-0.162961	-0.278061	-0.044889	-0.462351
LSCm < FC3	-0.808651	-0.034451	-0.101930	-0.200889	-0.178689
LSCm < APA	-0.751969	-0.454455	0.204995	0.023454	0.056127
COs < LSCm	-0.449476	-0.500247	0.027196	0.413073	0.138249

Measurement abbreviations as in Figure 1.

3.5. Principal components analysis

A PCA was carried out based on the shape indices of the canals and cochlea, the sagittal labyrinthine index, the proportion of each canal and the angular measures. The first five principal components showed eigenvalues >1.0 , indicating they explain more variation than any single variable in isolation, and together explain a total of 77.7% of the variance (Table 5). The first two principal components capture 45.1% of the variance and reflect the main taxonomic differences between samples.

The first principal component (PC1) explains 28.4% of the variance, with the SLI and three of the angular measures (LSCm < PpP, LSCm < FC3, LSCm < APA) showing the strongest (negative) correlations with PC1 (Table 5). Thus, individuals with lower values along PC1 tend to have a low placement of the posterior canal and higher angles between the lateral canal plane and other structures (Fig. 5). There is a good separation along PC1 between Neandertals, which cluster towards lower values, and modern humans, which show higher values. The Atapuerca (SH) sample falls somewhat in-between these two groups. Aroeira 3 falls outside the Neandertal and Atapuerca (SH) confidence ellipses, and clearly within the modern human range of variation along PC1.

The second principal component (PC2) explains 16.7% of the variance, and the proportions of the posterior and lateral canals show the strongest negative and positive correlations, respectively,

with PC2 (Table 5). Thus, individuals with high values along PC2 tend to show larger lateral canals and smaller posterior canals (Fig. 5). Along PC2, the Neandertals and modern humans show considerable overlap, while the Atapuerca (SH) sample shows higher values. The similar distribution of Neandertals and modern humans along PC2 cannot be explained only by the two variables showing the strongest correlations, since the Neandertals should fall towards higher values than modern humans given the differences in the canal proportions between these two groups. Nevertheless, their position along PC2 is also clearly influenced by the SLI

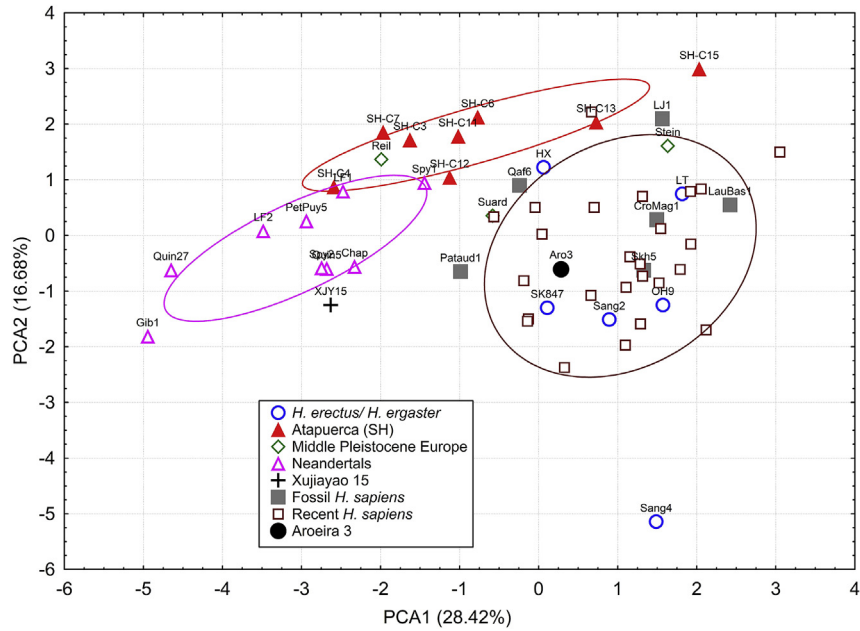


Figure 5. Results of the principal components analysis based on the correlation matrix of bony labyrinth variables that reflect the shape and spatial relationships of the semicircular canals and cochlea. The first two principal components (PC2 vs. PC1) are shown, as well as the 95% confidence ellipses for recent *H. sapiens*, Neandertals and the Atapuerca (SH) sample. The individual fossil specimens included in the analysis are labeled. Aroeira 3 clearly falls within the recent *H. sapiens* range of variation and outside of the Neandertal and Atapuerca (SH) confidence ellipses. Note also that nearly all the *H. ergaster/H. erectus* individuals fall within the recent *H. sapiens* confidence ellipse, suggesting the recent human bony labyrinth is largely primitive for the genus *Homo*.

and LSCm < APA, whose negative correlations with PC2, while lower (Table 5), compensate for the higher values of the Neandertals in the previous two variables, pushing them towards lower values along PC2. The elevated position of the Atapuerca (SH) individuals can be explained because they have similar canal proportions as the Neandertals, but unlike the Neandertals, they do not have high values in the SLI or the LSCm < APA. The position of Aroeira 3 along PC2 is within the range of variation of modern humans and Neandertals and outside the Atapuerca (SH) range of variation.

The remaining three principal components (PC3–PC5) explain an additional 32.6% of the variance (Table 5), but there is considerable overlap between all of the groups along all three PCs (SOM Figs. S1–S3).

The *H. ergaster/H. erectus* specimens, as well as the fossil specimens of *H. sapiens*, generally fall within, or very close to, the recent human 95% confidence ellipse, with the sole exception of Sangiran 4 (Fig. 5). This is also the case for two of the non-SH European Middle Pleistocene specimens (Steinheim and Abri Suard), while the third specimen (Reilingen) falls within the Atapuerca (SH) hominin confidence ellipse. Xujia Yao 15 falls very close to the Neandertal confidence ellipse, reflecting the Neandertal-like bony labyrinth morphology previously reported in this specimen (Wu et al., 2014). In sum, the results of the PCA separate the Neandertals, Atapuerca (SH) hominins and modern humans and clearly show that Aroeira 3 is included within the range of variation of modern humans.

3.6. Discriminant function analysis

DFA was carried out based on the same variables as the PCA (i.e., the shape indices of the canals and cochlea, the sagittal labyrinthine index, the proportion of each canal and the angular measures). Overall, the DFA correctly classified 87.5% of the individuals to their group (Table 6). All of the Atapuerca (SH) individuals (100%)

were correctly classified, followed by the recent *H. sapiens* (88%), *H. ergaster/H. erectus* (83.3%) and the Neandertals (77.8%). The posterior probabilities for the correctly classified individuals were generally high (>90%), although the probabilities range as low as 50.2% for one of the Atapuerca (SH) individuals (Cranium 12). Among the individual variables, several contribute most strongly to the discriminant function, including: LSCm < FC3, LSCm < FC4, SLI and LSCm < APA. Notably, all of these variables also show the strongest correlations with PC1 or PC2 in the PCA.

Aroeira 3 is classified nearly equally with both recent *H. sapiens* (47.2%) and *H. ergaster/H. erectus* (46.1%; Table 6), reflecting the similarity in bony labyrinth dimensions in these two groups. Although the posterior probabilities are not high for either classification, when combined, this suggests there is only a 6.5% chance of being classified with either the Atapuerca (SH) hominins or Neandertals. Among the other non-SH European Middle Pleistocene specimens, Reilingen is classified with the Atapuerca (SH) hominins, while Abri Suard is classified with Neandertals, both with high posterior probabilities. The classification of Steinheim is less clear, since this specimen is classified with *H. ergaster/H. erectus* and the Atapuerca (SH) hominins with nearly equal, but low, posterior probabilities. Finally, Xujia Yao 15 was classified with Neandertals, while a majority of the fossil *H. sapiens* individuals were classified with either recent *H. sapiens* or *H. ergaster/H. erectus* (Table 6).

4. Discussion

The results of the PCA revealed that most of the *H. ergaster/H. erectus* fossils fall within the *H. sapiens* range of variation, suggesting this likely represents the primitive condition for the genus *Homo*, as proposed in previous studies (Spoor et al., 2003; Quam et al., 2016). In contrast, potentially derived features in the Neandertal labyrinth include relatively large and small lateral and posterior canals, respectively, a relatively low position of the posterior

Table 6

Results of the discriminant function analysis based on bony labyrinth variables that reflect the shape and spatial relationships of the semicircular canals and cochlea.

Group (n)	% correctly classified ^a	<i>H. ergaster</i> / <i>H. erectus</i>	Atapuerca (SH)	Neandertals	Recent <i>H. sapiens</i>
<i>H. ergaster</i> / <i>H. erectus</i> (6)	83.3	5	1	0	0
Atapuerca (SH) (8)	100.0	0	8	0	0
Neandertals (9)	77.8	0	2	7	0
Recent <i>H. sapiens</i> (25)	88.0	2	1	0	22
Total (48)	87.5	7	12	7	22

Specimen	Classification	Posterior probabilities			
Aroeira 3	Recent <i>H. sapiens</i>	0.463	0.065	0.000	0.472
Abri Suard	Neandertals	0.001	0.017	0.982	0.000
Reilingen	Atapuerca (SH)	0.009	0.988	0.002	0.001
Steinheim	<i>H. ergaster</i> / <i>H. erectus</i>	0.363	0.334	0.019	0.284
Xujiayao 15	Neandertals	0.002	0.098	0.899	0.000
Liujiang 1	Atapuerca (SH)	0.160	0.823	0.000	0.017
Qafzeh 6	Atapuerca (SH)	0.076	0.918	0.000	0.006
Skhul 5	<i>H. ergaster</i> / <i>H. erectus</i>	0.981	0.001	0.001	0.018
Abri Pataud 1	<i>H. ergaster</i> / <i>H. erectus</i>	0.959	0.020	0.000	0.020
Cro Magnon 1	<i>H. ergaster</i> / <i>H. erectus</i>	0.891	0.010	0.000	0.099
Laugerie Basse 1	Recent <i>H. sapiens</i>	0.096	0.010	0.000	0.894

^a Assumes equal prior probabilities of group membership.

canal and differences in the angular relationships between the lateral canal plane and several structures of the temporal bone (Spoor et al., 2003). The PCA shows Aroeira 3 falling with fossil and recent *H. sapiens* individuals and outside the confidence ellipses for Neandertals and the Atapuerca (SH) hominins, and the DFA classified Aroeira 3 fairly evenly with recent *H. sapiens* and *H. ergaster*/*H. erectus*. Thus, the present study of the bony labyrinth in Aroeira 3 suggests that this individual was characterized by a morphology that is largely primitive for the genus *Homo*.

Regarding the derived features in the Neandertal bony labyrinth, the relatively large lateral canal has been argued to reflect their large body mass (Spoor et al., 2003), and the observed mean size of the lateral canal in Neandertals is similar to that predicted from their body mass and agility (Spoor et al., 2007). The remaining derived features in Neandertals have been argued to reflect a hyperrotation of the cranial base associated with large brain size and a platycephalic brain shape (Spoor et al., 2003). This suggestion is consistent with the difference in allometric trends in encephalization that have been reported to characterize modern humans and Neandertals (Bruner et al., 2003). More recently, the bony labyrinth morphology in *H. sapiens* has been shown to covary with the surrounding cranial base (Gunz et al., 2013). In particular, individuals with wider cranial bases, particularly the posterior cranial fossa, were shown to have relatively smaller and low-placed posterior canals. Thus, the distinctive Neandertal morphology may be partly related to the combination of absolutely large body and brain size and an archaic brain shape and pattern of expansion. However, differences in the bony labyrinth morphology between Neandertals and modern humans cannot be fully explained by this pattern of covariation (Gunz et al., 2013), suggesting the possibility of some functional differences and indicating that variation in the bony labyrinth does retain a phylogenetic signal.

The Atapuerca (SH) hominins are the earliest fossils to show clearly derived Neandertal features in the cranium (Arsuaga et al., 1997) and temporal bone (Martínez and Arsuaga, 1997), and are considered broadly ancestral to the more recent Neandertals (Arsuaga et al., 2014). Analysis of the Atapuerca (SH) bony labyrinth revealed that the derived canal proportions seen in Neandertals are already present at this early stage (Quam et al., 2016), and this is one of the first Neandertal features to appear close to the origin of the Neandertal clade.

In contrast, the posterior canal in the Atapuerca (SH) hominins is not in a low position relative to the lateral canal, differing

from the Neandertals in this regard. The limited data available for other European Middle Pleistocene fossils indicate that these individuals also show the derived canal proportions seen in the Atapuerca (SH) hominins and Neandertals. In terms of the relative position of the posterior canal, only the specimen from Reilingen shows a low-placed posterior canal. The chronology for Reilingen is uncertain and may range from MIS 9 to MIS 11, making it slightly younger than the Iberian fossils from Atapuerca (SH) and Aroeira, to MIS 5e, near the beginning of the Late Pleistocene and contemporaneous with Neandertals (Ziegler and Dean, 1998). Thus, changes in canal proportions seem to have preceded the shift in the relative position of the posterior canal (i.e., high SLI), which may be related to further increases in absolute brain size.

The correlation between absolute brain size and bony labyrinth morphology is not straightforward, since even some relatively small-brained Neandertal individuals show a derived bony labyrinth. Within the Atapuerca (SH) sample, there is no clear correlation between bony labyrinth dimensions and brain size, since larger-brained individuals are not more Neandertal-like in their bony labyrinth. Nevertheless, this pattern of covariation may partially explain the presence of derived Neandertal features in the bony labyrinths of several Late Pleistocene crania from China, some of which have very large cranial capacities (>1700 mm³) and wide cranial bases (Li et al., 2017). The brain size in Aroeira 3 is difficult to estimate precisely, due to its incomplete state of preservation, but has been suggested to fall between 1200 and 1400 mm³, similar to the range of variation in the Atapuerca (SH) sample (Daura et al., 2017). Thus, the bony labyrinth differences between the Atapuerca (SH) hominins and Aroeira 3 are not attributable to differences in brain size.

The bony labyrinth in Aroeira 3 shows neither the derived canal proportions nor low placement of the posterior canal seen in Neandertals. In these features, the Aroeira 3 individual is largely primitive for the genus *Homo* and less derived towards the Neandertal condition than the Atapuerca (SH) sample and most other European Middle Pleistocene specimens. Nevertheless, one potentially derived feature is shared between Aroeira 3 and the Atapuerca (SH) sample: the shape index of the cochlear basal turn is low, reflecting a relative shortening of the height of the basal turn. While low values for this index can also be found in some *H. ergaster*/*H. erectus* individuals, the value for this index in Aroeira 3 falls outside of the range of variation in all of the fossil

comparative samples, except for Atapuerca (SH), and is only higher than one individual from our recent *H. sapiens* sample.

4.1. Cranial, temporal bone and labyrinthine morphology

The finding of a largely primitive bony labyrinth in Aroeira 3 can be considered in light of the morphology of the cranium and temporal bone (Daura et al., 2017). Based on the morphology of the supraorbital torus, particularly the better preserved glabellar region, Aroeira 3 was argued to resemble the Atapuerca (SH), Steinheim and Petralona specimens. In addition, the supraorbital arches, while abraded in Aroeira 3, were said to show a rounded anterior surface, again resembling these same fossils. In both these aspects of the supraorbital torus morphology, Aroeira 3 differs from the Arago and Ceprano fossils. Unfortunately, since these last two fossils lack a temporal bone, no information on their bony labyrinth morphology is available.

Like the bony labyrinth, the petromastoid region of the temporal bone in Neandertals is also characterized by a suite of derived features (Martínez and Arsuaga, 1997; Dean et al., 1998), including: (1) a mastoid process that shows little projection below the cranial base and whose apex is directed medially; (2) the presence of an anterior mastoid tubercle on the anterolateral face of the mastoid process; (3) the presence of a well-developed juxtamastoid eminence; (4) the base of the styloid process is medially placed with respect to the stylomastoid foramen and the digastric groove; and (5) the anterior portion of the digastric groove is separated from the stylomastoid foramen by a bony bridge. In addition, the glenoid fossa in Neandertals also shows a derived morphology, with a well-developed postglenoid process posteriorly and, more importantly, a flattened articular eminence anteriorly (Martínez and Arsuaga, 1997).

The mastoid region in the Atapuerca (SH) sample is largely primitive in showing large, projecting mastoid processes, an uninterrupted digastric groove that is aligned with the base of the styloid process, and absence of the anterior mastoid tubercle. The Aroeira 3 temporal bone also shows a largely primitive (i.e., non-Neandertal) mastoid region (Daura et al., 2017), similar to the Atapuerca (SH) hominins and other European Middle Pleistocene fossils. While the mastoid process in Aroeira 3 is small, it is well individualized from the occipitomastoid region and projects posteriorly without any medial inclination of the apex. Similarly small (non-projecting) mastoid processes can be found in Atapuerca (SH) Crania 7 and 12 (both considered adults), Reilingen and Steinheim (Martínez and Arsuaga, 1997; Dean et al., 1998).

Regarding the glenoid fossa, Aroeira 3 shows a well-developed and triangular postglenoid process posteriorly. Although the apex of the process is damaged in Aroeira 3, its minimum mediolateral (29 mm) and superoinferior (13 mm) dimensions are similar to values seen in the Atapuerca (SH) sample, and these latter hominins show the largest postglenoid processes in the genus *Homo* (Martínez and Arsuaga, 1997; Martínez et al., 2008). A well-developed postglenoid process is characteristic of both European Middle Pleistocene fossils and Neandertals (Martínez and Arsuaga, 1997; Arsuaga et al., 2014). However, the shape of the process in Neandertals can vary between triangular (e.g., Krapina) and more trapezoidal, with a truncated triangular apex (e.g., La Quina H5, La Ferrassie 1 and La Chapelle-aux-Saints 1; Vallois, 1969; Heim, 1974).

Aroeira 3 does not show a flattened articular eminence (Daura et al., 2017), differing from the Atapuerca (SH) fossils and other European Middle Pleistocene specimens where this feature can be observed, as well as Neandertals (Martínez and Arsuaga, 1997; Martínez et al., 2008; Arsuaga et al., 2014). Importantly, this is one of the earliest derived Neandertal features seen in the fossil record, the presence of this morphology being tied to the

emergence of a masticatory specialization near the origin of the Neandertal clade (Arsuaga et al., 2014). Thus, the absence of this feature in Aroeira 3 indicates a more primitive morphology. Nevertheless, the articular eminence in Aroeira 3 is similar to one of the Atapuerca (SH) individuals (temporal bone AT-84, associated with Atapuerca [SH] Cranium 12).

Aroeira 3 overall combines a primitive bony labyrinth and temporal bone anatomy, with the sole possible exception of the well-developed postglenoid process. In contrast, the Atapuerca (SH) hominins and most other European Middle Pleistocene specimens share a derived glenoid cavity morphology with Neandertals, together with a bony labyrinth that also shows some Neandertal derived features. Thus, it may be tempting to view the derived canal proportions as related to the emergence of the derived glenoid fossa morphology, although the basis for such a link is unclear. Nevertheless, the AT-84 specimen combines a glenoid fossa morphology similar to that seen in Aroeira 3, but still shows the derived canal proportions of Neandertals.

4.2. Evolutionary implications

The implications of the bony labyrinth morphology in Aroeira 3 can be considered within current ideas about the evolutionary process during the Middle Pleistocene in Europe. The 'Neandertal accretion model' posits a gradual emergence of Neandertal features during the course of the Middle Pleistocene, with increasingly Neandertal-derived populations appearing through time (Dean et al., 1998; Hublin, 1998, 2009; Arsuaga et al., 1997, 2014). Nevertheless, it has proven difficult to arrange the Middle Pleistocene specimens into a chronological sequence that reveals a consistent pattern to the emergence of Neandertal features. Rather, some specimens that appear more derived toward Neandertals, such as the Atapuerca (SH) hominins, are older than others that lack clear Neandertal features, such as Ceprano (Manzi et al., 2010; Arsuaga et al., 2014). While the Neandertal accretion model is compatible with either an anagenetic or cladogenetic evolutionary pattern, the morphological variability in the European fossil record has led to recognition that a linear evolutionary model is not compatible with the fossil evidence, and that there is likely more than one lineage represented during the European Middle Pleistocene (Tattersall, 2011; Stringer, 2012; Arsuaga et al., 2014; Manzi, 2016).

An alternative approach underlines the importance of population dynamics below the species rank (paleodemes sensu Howell, 1999) and the effects of environmental changes and geography (Hublin, 1998, 2009; Dennell et al., 2011; Bermúdez de Castro and Martínón-Torres, 2013). In contrast to habitat-tracking models, which posit large-scale north-south population migrations based on changing climatic conditions, these approaches rely on population expansion and contraction and frequent extinctions of local groups as a result of climatic deterioration. Models such as these, based on demographic factors, share many elements with the standard allopatric speciation model and are underpinned by a sound theoretical basis (Coyne and Orr, 2004). Indeed, speciation during hominin evolution, including the European Middle Pleistocene, is often explicitly modeled as allopatric (Tattersall, 1992, 2011).

In particular, the model proposed by Dennell et al. (2011) for Middle Pleistocene Europe posits more or less stable populations and continuous human occupation in the southern portion of Europe, including the Iberian Peninsula. During warmer Marine Isotope Stages (MIS), representing milder climatic conditions, the paleodeme size increases and the geographic range expands into more northern latitudes. During more adverse conditions, represented by colder isotope stages, these northern populations reduce in size and fracture into isolated local populations that are often

demographically unstable and frequently disappear completely. Those that do survive are largely restricted to refugium areas, whose location and extension vary in function of the geography of each region, and in which isolating mechanisms, including genetic drift and founder effects, can be most important. Thus, this isolation can lead to the extinction of many of these local populations as well as to the appearance of endemic, derived (autapomorphic) features and the fixation of particular combinations of features by genetic drift.

According to the aforementioned model, when the climatic conditions improve and return to being favorable during the warm isotopic stages, the isolated local populations expand demographically and geographically again, including from the more stable southern regions. This situation favors the contact and hybridization between surviving populations and gives rise to new paleodemes with new combinations of features (Dennell et al., 2011). This model can explain the morphological diversity that is documented in the European Middle Pleistocene and the existence of roughly contemporaneous fossils with different combinations of primitive and derived features, such as is the case of the Arago and Atapuerca (SH) fossil samples (Arsuaga et al., 2014; Bermúdez de Castro et al., 2018).

While these models generally apply to populations occupying more northerly latitudes, where climatic fluctuations can be expected to be more extreme, similar demographic processes may have also characterized the southern regions of Europe, including the Iberian Peninsula, during particularly cold isotope stages. The present study has revealed that the bony labyrinth morphology in Aroeira 3 is more primitive than in the Atapuerca (SH) hominins, indicating an important degree of demographic isolation between these roughly coeval Iberian populations. At the same time, Aroeira 3 shares an apparently derived feature, the shape of the cochlear basal turn, with the Atapuerca (SH) fossils, suggesting the existence of an earlier Iberian paleodeme, from which both populations inherited this feature.

It is important to point out that both sites are dated around the MIS 12/MIS 11 transition. MIS 12 is one of the coldest and least favorable periods for European Middle Pleistocene populations (MacDonald et al., 2012), while MIS 11 is considered a particularly warm and favorable period, comparable with the environmental conditions in the Holocene (Hublin, 2009). In this context, it is reasonable to suggest that Aroeira 3 and the Atapuerca (SH) hominins derive from a wider paleodeme that inhabited the Iberian Peninsula during MIS 13, a warm period favorable for population expansion. Later, the worsening conditions during MIS 12, combined with the geographic and topographic variation of the Iberian Peninsula, would have precipitated the fragmentation of the original Iberian paleodeme into small isolated populations that preserved features in common from the original paleodeme, such as the shape of the cochlear basal turn, or the morphology of the glabellar region and the well-developed postglenoid process in the cranium.

The derived cochlear shape would have been subsequently lost during the Middle Pleistocene, since it is generally absent in Neandertals. The disappearance of this feature may plausibly be linked to these same processes of population expansion and fragmentation during alternating warm and cold periods at some point after the time of the Atapuerca (SH) hominins. Among other European Middle Pleistocene crania, the derived cochlear shape is present only in Reilingen.

Models based on demographic factors, such as that of Dennell et al. (2011), have the advantage of proposing concrete evolutionary hypotheses to explain the distribution of features in different fossils. Based on the distribution of features observed in Aroeira 3 and the Atapuerca (SH) population, we predict the

existence of a paleodeme in the Iberian Peninsula during MIS 13 that would have been characterized, at least, by the presence of a prominent glabellar region, a well-developed postglenoid process and a low shape index of the cochlear basal turn. Both Aroeira 3 and the Atapuerca (SH) hominins would have inherited these features from this earlier paleodeme. Future discoveries of fossils at different sites from this region and time period will make it possible either to confirm or reject the hypotheses proposed here.

5. Conclusions

The study of the bony labyrinth in the Middle Pleistocene Aroeira 3 cranium has revealed the absence of Neandertal-derived features. This specimen therefore contrasts with other European Middle Pleistocene fossils, including the roughly contemporaneous Atapuerca (SH) hominins. Instead, Aroeira 3 shows a largely primitive bony labyrinth, more similar to earlier members of the genus *Homo*. The cranial anatomy and bony labyrinth morphology provide new insights into the population dynamics in Middle Pleistocene Europe, suggesting a degree of demographic isolation even among geographically and chronologically close populations.

Acknowledgments

The authors thank the associate editor and the two anonymous reviewers for their insightful and constructive comments on improving the manuscript. This research has been supported by the Ministerio de Economía y Competitividad of the Spanish Government (Projects 2017SGR-00011, HAR2017-86509 and CGL2015-65387-C3-2-P [MINECO/FEDER]). Fieldwork at the Gruta da Aroeira was funded by the Câmara Municipal de Torres Novas and Fundação para a Ciência e Tecnologia with logistical support by Fábrica de Papel A Renova. M.C.V. has been supported by a predoctoral grant from the Fundación Atapuerca, R.M.Q. by Programa 'Ginés de los Ríos' (Universidad de Alcalá), J.D. by a Ramón y Cajal grant (RYC-2015-17667), and M.S. by a Juan de la Cierva postdoctoral grant (FJCI-2014-21386). This paper is the result of research performed by the Evolutionary Bioacoustics Group at the Universidad de Alcalá (Spain).

Supplementary Online Material

Supplementary online material related to this article can be found at

References

- Antón, S., 2003. Natural history of *Homo erectus*. *Yearbook of Physical Anthropology* 46, 126–170.
- Arsuaga, J.L., Martínez, I., Gracia, A., Lorenzo, C., 1997. The Sima de los Huesos crania (Sierra de Atapuerca, Spain). A comparative study. *Journal of Human Evolution* 33, 219–281.
- Arsuaga, J.L., Martínez, I., Arnold, L., Aranburu, A., Gracia-Téllez, A., Sharp, W., Quam, R., Falguères, C., Pantoja-Pérez, A., Bischoff, J., Poza-Rey, E., Parés, J., Carretero, J., Demuro, M., Lorenzo, C., Sala, N., Martín-Torres, M., García, N., Alcázar de Velasco, A., Cuenca-Bescós, G., Gómez-Olivencia, A., Moreno, D., Pablos, A., Shen, C., Rodríguez, L., Ortega, A., García, R., Bonmatí, A., Bermúdez de Castro, J.M., Carbonell, E., 2014. Neandertal roots: cranial and chronological evidence from Sima de los Huesos. *Science* 344, 1358–1363.
- Bermúdez de Castro, J.M., Martín-Torres, M., 2013. A new model for the evolution of the human Pleistocene populations of Europe. *Quaternary International* 295, 102–112.
- Bermúdez de Castro, J.M., Martín-Torres, M., de Pinillos, M.M., García-Campos, C., Modesto-Mata, M., Martín-Francés, L., Arsuaga, J.L., 2018. Metric and morphological comparison between the Arago (France) and Atapuerca-Sima de los Huesos (Spain) dental samples, and the origin of Neanderthals. *Quaternary Science Reviews*. <https://doi.org/10.1016/j.quascirev.2018.04.003>.
- Bouchneb, L., Crevecoeur, I., 2009. The inner ear of Nazlet Khater 2 (Upper Paleolithic, Egypt). *Journal of Human Evolution* 56, 257–262.

- Bruner, E., Manzi, G., Arsuaga, J., 2003. Encephalization and allometric trajectories in the genus *Homo*: evidence from the Neandertal and modern lineages. Proceedings of the National Academy of Sciences USA 100, 15335–15340.
- Coyne, J.A., Orr, H.A., 2004. Speciation. Sinauer, Sunderland.
- Daura, J., Sanz, M., Arsuaga, J.L., Hoffmann, D.L., Quam, R.M., Ortega, M.C., Santos, E., Gómez, S., Rubio, A., Villaescusa, L., Souto, P., Mauricio, J., Rodrigues, F., Ferreira, A., Godinho, P., Trinkaus, E., Zilhão, J., 2017. New Middle Pleistocene hominin cranium from Gruta da Aroeira (Portugal). Proceedings of the National Academy of Sciences USA 114, 3397–3402.
- Daura, J., Sanz, M., Deschamps, M., Matias, H., Igreja, M., Villaescusa, L., Gómez, S., Rubio, A., Souto, P., Rodrigues, F., Zilhão, J., 2018. The 400,000 year-old Acheulean assemblage associated with the Aroeira-3 human cranium (Gruta da Aroeira, Almonda karst system, Portugal). Comptes Rendus Palevol. <https://doi.org/10.1016/j.crpv.2018.03.003>.
- Dean, D., Hublin, J., Holloway, R., Ziegler, R., 1998. On the phylogenetic position of the pre-Neandertal specimen from Reilingen, Germany. Journal of Human Evolution 34, 485–508.
- de Lumley, M.A., 2015. L'homme de Tautavel. Un *Homo erectus* européen évolué. *Homo erectus tautavelensis*. L'Anthropologie (Paris) 119, 303–348.
- Dennell, R.W., Martínón-Torres, M., Bermúdez de Castro, J.M., 2011. Hominin variability, climatic instability and population demography in Middle Pleistocene Europe. Quaternary Science Reviews 30, 1511–1524.
- Gilbert, W., Holloway, R., Kubo, D., Kono, R., Suwa, G., 2008. Tomographic analysis of the Daka calvaria. In: Gilbert, W., Asfaw, B. (Eds.), *Homo erectus*. Pleistocene Evidence from the Middle Awash, Ethiopia. University of California Press, Berkeley, pp. 329–348.
- Glantz, M., Viola, B., Wrinn, P., Chikisheva, T., Derevianko, A., Krivoschapkin, A., Islamov, U., Suleimanov, R., Ritzmann, T., 2008. New hominin remains from Uzbekistan. Journal of Human Evolution 55, 223–237.
- Gómez-Olivencia, A., Crevecoeur, I., Balzeau, A., 2015. La Ferrassie 8 Neandertal child reloaded: new remains and re-assessment of the original collection. Journal of Human Evolution 82, 107–126.
- Guipt, G., de Lumley, M.-A., Tuffreau, A., Mafart, B., 2011. A late Middle Pleistocene hominid: Biache-Saint-Vaast 2, north France. Comptes Rendus Palevol 10, 21–33.
- Gunz, P., Stoessel, A., Neubauer, S., Kuhrig, M., Hoyka, M., Hublin, J.-J., Spoor, F., 2013. Morphological integration of the bony labyrinth and the cranial base in modern humans and Neandertals. Proceedings of the European Society for the Study of Human Evolution 5, 104.
- Heim, J.L., 1974. Les Hommes fossiles de la Ferrassie (Dordogne) et le problème de la définition des Neandertaliens classiques. L'Anthropologie 78, 321–377.
- Hill, C.A., Radović, J., Frayer, D.W., 2014. Brief communication: Investigation of the semicircular canal variation in the Krapina Neandertals. American Journal of Physical Anthropology 154, 302–306.
- Howell, F.C., 1999. Paleo-demes, species clades, and extinctions in the Pleistocene hominin record. Journal of Anthropological Research 55, 191–243.
- Hublin, J.J., 1998. Climatic changes, paleogeography, and the evolution of the Neandertals. In: Akazawa, T., Aoki, K., Bar-Yosef, O. (Eds.), Neandertals and Modern Humans in Western Asia. Plenum Press, New York, pp. 295–310.
- Hublin, J.J., 2009. The origin of Neandertals. Proceedings of the National Academy of Sciences USA 106, 16022–16027.
- Hublin, J.J., Spoor, F., Braun, M., Zonneveld, F., Condemi, S., 1996. A late Neandertal associated with Upper Paleolithic artefacts. Nature 381, 224–226.
- Kachigan, S., 1991. Multivariate Statistical Analysis. A Conceptual Introduction, 2nd ed. Radius Press, New York.
- Li, Z.-Y., Wu, X.-J., Zhou, L.-P., Liu, W., Gao, X., Nian, X.-M., Trinkaus, E., 2017. Late Pleistocene archaic human crania from Xuchang, China. Science 355, 969–972.
- MacDonald, K., Martínón-Torres, M., Dennell, R.W., Bermúdez de Castro, J.M., 2012. Discontinuity in the record for hominin occupation in south-western Europe: implications for occupation of the middle latitudes of Europe. Quaternary International 271, 84–97.
- Manzi, G., 2016. Humans of the Middle Pleistocene: the controversial calvarium from Ceprano (Italy) and its significance for the origin and variability of *Homo heidelbergensis*. Quaternary International 411, 254–261.
- Manzi, G., Magri, D., Milli, S., Palombo, M., Margari, V., Celiberti, V., Barbieri, M., Barbieri, M., Melis, R., Rubini, M., Ruffo, M., Saracino, B., Tzedakis, P., Zarattini, A., Biddittu, I., 2010. The new chronology of the Ceprano calvarium (Italy). Journal of Human Evolution 59, 580–585.
- Marks, A.E., Brugal, J.P., Chabai, V.P., Monigal, K., Goldberg, P., Hockett, B., Peman, E., Elorza, M., Malloll, C., 2002a. Le gisement Pléistocène moyen de Galeria Pesada (Estrémadura, Portugal): premiers résultats. Paléo 14, 77–100.
- Marks, A.E., Monigal, K., Chabai, V.P., Brugal, J.P., Goldberg, P., Hockett, B., Peman, E., Elorza, M., Malloll, C., 2002b. Excavations at the Middle Pleistocene Cave site of Galeria Pesada, Portuguese Estremadura: 1997–1999. O Arqueólogo Português 20, 7–38.
- Martínez, I., Arsuaga, J.L., 1997. The temporal bones from Sima de los Huesos Middle Pleistocene site (Sierra de Atapuerca, Spain). A phylogenetic approach. Journal of Human Evolution 33, 283–318.
- Martínez, I., Quam, R., Arsuaga, J.L., 2008. Evolutionary trends in the temporal bone in the Neandertal lineage: a comparative study between the Sima de los Huesos (Sierra de Atapuerca) and Krapina samples. In: Monge, J., Mann, A., Frayer, D.W., Radović, J. (Eds.), New Insights on the Krapina Neandertals: 100 Years after Gorjanović-Kramberger. Croatian Natural History Museum, Zagreb, pp. 75–83.
- Meyer, M., Arsuaga, J.L., de Filippo, C., Nagel, S., Aximu-Petri, A., Nickel, B., Martínez, I., Gracia, A., Bermúdez de Castro, J.M., Carbonell, E., 2016. Nuclear DNA sequences from the Middle Pleistocene Sima de los Huesos hominins. Nature 531, 504–507.
- Ponce de León, M., Zollikofer, C., 2010. The labyrinthine morphology. In: Doboş, A., Soficaru, A., Trinkaus, E. (Eds.), The Prehistory and Paleontology of the Peştera Muierii, Romania. Études et Recherches Archéologiques de l'Université de Liège, Liège, pp. 96–97.
- Ponce de León, M., Zollikofer, C., 2013. The internal cranial morphology of Oase 2. In: Trinkaus, E., Constantin, S., Zilhão, J. (Eds.), Life and Death at the Peştera cu Oase. A Setting for Modern Human Emergence in Europe. Oxford University Press, New York, pp. 332–347.
- Ponce de León, M.S., Koesbardiati, T., Weissmann, J.D., Milella, M., Reyna-Blanco, C.S., Suwa, G., Kondo, O., Malaspina, A.-S., White, T.D., Zollikofer, C.P., 2018. Human bony labyrinth is an indicator of population history and dispersal from Africa. Proceedings of the National Academy of Sciences USA 115, 4128–4133.
- Quam, R., Lorenzo, C., Martínez, I., Gracia-Téllez, A., Arsuaga, J.L., 2016. The bony labyrinth of the middle Pleistocene Sima de los Huesos hominins (Sierra de Atapuerca, Spain). Journal of Human Evolution 90, 1–15.
- Rightmire, G.P., 1990. The Evolution of *Homo erectus*. Cambridge University Press, Cambridge.
- Rightmire, G.P., 2008. *Homo* in the Middle Pleistocene: hypodigms, variation, and species recognition. Evolutionary Anthropology 17, 8–21.
- Roksandic, M., Mihailović, D., Mercier, N., Dimitrijević, V., Morley, M., Rakočević, Z., Mihailović, B., Guibert, P., Babb, J., 2011. A human mandible (BH-1) from the Pleistocene deposits of Mala Balanica cave (Sićevo Gorge, Niš, Serbia). Journal of Human Evolution 61, 186–196.
- Spoor, F., 1993. The comparative morphology and phylogeny of the human bony labyrinth. Ph.D. Dissertation, Utrecht University.
- Spoor, F., Esteves, F., Tecelão Silva, F., Pacheco Dias, R., 2002. The bony labyrinth of Lagar Velho 1. In: Zilhão, J., Trinkaus, E. (Eds.), Portrait of the Artist as a Child. The Gravettian Human Skeleton from the Abrigo do Lagar Velho and its Archaeological Context, Trabalhos de Arqueologia, vol. 22, pp. 287–292.
- Spoor, F., Hublin, J., Braun, M., Zonneveld, F., 2003. The bony labyrinth of Neandertals. Journal of Human Evolution 44, 141–165.
- Spoor, F., Garland, T., Krovitz, G., Ryan, T.M., Silcox, M.T., Walker, A., 2007. The primate semicircular canal system and locomotion. Proceedings of the National Academy of Sciences USA 104, 10808–10812.
- StatSoft, 2010. Statistica 10.0. StatSoft, Tulsa.
- Stringer, C., 2012. The status of *Homo heidelbergensis* (Schoetensack 1908). Evolutionary Anthropology: Issues, News, and Reviews 21, 101–107.
- Stringer, C., Hublin, J., 1999. New age estimates for the Swanscombe hominid, and their significance for human evolution. Journal of Human Evolution 37, 873–877.
- Tattersall, I., 1992. Species concepts and species identification in human evolution. Journal of Human Evolution 22, 341–349.
- Tattersall, I., 2007. *Homo ergaster* and its contemporaries. In: Henke, W., Tattersall, I. (Eds.), Handbook of Paleoanthropology. Springer-Verlag, Berlin/Heidelberg, pp. 1633–1653.
- Tattersall, I., 2011. Before the Neanderthals: hominid evolution in Middle Pleistocene Europe. In: Condemi, S., Weniger, G.C. (Eds.), Continuity and Discontinuity in the Peopling of Europe. Springer, Dordrecht, pp. 47–53.
- Trinkaus, E., Marks, A., Brugal, J., Bailey, S., Rink, W., Richter, D., 2003. Later Middle Pleistocene human remains from the Almonda Karstic system, Torres Novas, Portugal. Journal of Human Evolution 45, 219–226.
- Uhl, A., Reyes-Centeno, H., Grigorescu, D., Kranjčič, E.F., Harvati, K., 2016. Inner ear morphology of the Cioclovina early modern European calvaria from Romania. American Journal of Physical Anthropology 160, 62–70.
- Vallois, H.V., 1969. Le temporal néandertalien H 27 de La Quina. Étude anthropologique. L'Anthropologie 5–6, 365–400.
- Wood, B., 1991. Koobi Fora Research Project, Vol. 4. In: Hominid Cranial Remains. Clarendon Press, Oxford.
- Wu, X.J., Crevecoeur, I., Liu, W., Xing, S., Trinkaus, E., 2014. Temporal labyrinths of eastern Eurasian Pleistocene humans. Proceedings of the National Academy of Sciences USA 111, 10509–10513.
- Ziegler, R., Dean, D., 1998. Mammalian fauna and biostratigraphy of the pre-Neandertal site of Reilingen, Germany. Journal of Human Evolution 34, 469–484.